European Conference on Computational Fluid Dynamics
ECCOMAS CFD 2006
P. Wesseling, E. Oñate and J. Périaux (Eds)

EVALUATION OF AERODYNAMIC NOISE GENERATION: PARAMETER STUDY OF A GENERIC SIDE MIRROR EVALUATING THE AEROACOUSTIC SOURCE STRENGTH

Thorsten Grahs* **and Carsten Othmer†**

* E2KB – Body design analysis,
Letter box 1537,
e-mail: thorsten.grahs@volkswagen.de
† E1KB – Body design analysis,
Letter box 1697
e-mail: carsten.othmer@volkswagen.de

Technical Development, Volkswagen AG, D-38436 Wolfsburg, Germany

Key words: aero acoustics, automotive applications, side mirror, DES, SAS

Abstract. *Based on a simple generic side mirror geometry, well featured with detailed measurements, we examine different combinations of meshing strategies and turbulence model, nameley DES (Detached Eddy Simulation) and SAS (Scale Adaptive Simulation).*

The best combination of this investigation is applied to some modified mirror geometries, in order to develop and evaluate a ranking process for the noise generation of the distinct side mirror geometries. Starting from the working knowledge of the design department, we focus on three modified geometries, with reveals good and bad properties in terms of noise production.

Thus, we take one geometry with all good properties, one with all poor properties and one in-between. The question is, whether we are able to reproduce this knowledge with our computational process. Since we are dealing with industrial application and due to the time consuming computations, not suitable for an rapid development process we focus more on the possibility to classifiy the noisyness of a part rather than detailed physicall modelling. This is due to the fact, that we have to deal with evaluation times of hours or days, rather than weeks or months, which a detailed LES (Large Eddy Simulation) or well resolved DES/SAS computation will last.

1 INTRODUCTION

Over the last years, the field of Computational Aero Acoustics (CAA) became more and more relevant for the industrial applications. The rapid development of computational power and modelling lead to the opportunity of thinking about aero acoustics computation in the virtual development process.

Already common in the area of the aero space industry, the generation of noise also become more and more relevant in the car development process. Stream induced noise, generated by add-on parts at the vehicle body, i.e. side mirrors, antennas or spoilers, are important, concerning the comfort results for the driver. Also such part like sun roofs and in this context the generation of sun-roof-buffeting is an important issue for the early development process, and so especially for the simulation.

Since this simulation task is both, new and difficult, we start our examination from a simple and well known test case to develop a computational strategy for the simulation of noise generated by side mirror geometries. Emphasise is given to the evaluation process to find a suitable way to estimate the loudness of an add-on part and to be able to rank different geometries.

The paper is organised as follow. First, we are going to discuss the equations and terms, which are relevant for the generation of aero acoustic noise. Than we estimate the noise sources to get a hint which are the dominant phenomena which occur. Different mesh strategies and turbulence models are examined and base on this results, the geometry variants are computed. To these data we apply an evaluation process to estimate the geometries. The results are reported and finally, conclusions are drawn.

2 Governing Equations

The area of aero acoustics is deeply combined with the name of Lighthill, which he pioneered with his first paper[1]. There, starting from the Navier-Stokes Equation he rewrites them and derives one scalar equation for the propagation of sound.

To repeat this proceeding shortly, Lighthill used the continuity equation

$$\frac{\partial \rho}{\partial t} + \frac{\partial \rho u_i}{\partial x_i} = 0, \tag{1}$$

and the momentum equation

$$\frac{\partial \rho u_i}{\partial t} + \frac{\partial \rho u_i u_j}{\partial x_j} = -\frac{\partial p}{\partial x_i} + \frac{\partial \tau_{ij}}{\partial x_j}, \tag{2}$$

where

$$\tau_{ij} = \mu\left(\frac{\partial u_i}{\partial x_j} + \frac{\partial u_j}{\partial x_i} - \frac{2}{3}\frac{\partial u_k}{\partial x_k}\delta_{ij}\right)$$

is the viscous stress tensor for a Newtonian fluid.

Differentiating (1) with respect to time, in order to derive an wave equation like operator, and subtracting the divergence of (2) leads to an scalar equation of the form

$$\frac{\partial^2 \rho}{\partial t^2} - \frac{\partial^2 \rho u_i u_j}{\partial x_i \partial x_j} = \frac{\partial^2 p}{\partial x_i^2} - \frac{\partial^2 \tau_{ij}}{\partial x_i \partial x_j}.$$

Moving the convective term to the right hand side and adding an additional term $-c^2\partial^2\rho/\partial x_i^2$ on both side, one gets a wave equation for the density, i.e.

$$\frac{\partial^2\rho}{\partial t^2} - c^2\frac{\partial^2\rho}{\partial x_i^2} = \frac{\partial^2 T_{ij}}{\partial x_i \partial x_j}. \tag{3}$$

Here, $T_{ij} = \rho u_i u_j - \tau_{ij} + (p - c^2\rho)\delta_{ij}$ is called the *Lighthill tensor*, and c is the speed of sound. The Equation (3) is well known as *Lighthill's Equation*.

An extension of this approach, to the presence of solid surfaces was first done by Curle[2] and later extended by Ffwocs Williams and Hawkings[3] to surfaces in arbitrary motion. There equation reads as

$$\frac{\partial^2\rho}{\partial t^2} - c^2\frac{\partial^2\rho}{\partial x_i^2} = \frac{\partial}{\partial t}\left\{\rho_0 v_n \delta(f)\right\} - \frac{\partial}{\partial x_i}\left\{p_{ij}\delta(f)\right\} + \frac{\partial^2 T_{ij}}{\partial x_i \partial x_j}, \tag{4}$$

where the source terms on the right-hand side describe monopole, dipole and quadrapole terms, respectively. For a stationary surface, one can neglect the monopole terms.

Doing this, we compare the dipole and quadrapole terms. The intensity for dipole term is proportional to the flow velocity i.e.

$$I_D \approx \rho u^6 c^{-3} l^2, \tag{5}$$

and for the quadrapole term

$$I_Q \approx \rho u^8 c^{-5} l^2. \tag{6}$$

Thus, comparing (5) and (6), we get for the ratio of both

$$\frac{I_Q}{I_D} \sim \left(\frac{u}{c}\right)^2.$$

Considering a Mach number $Ma = u/c$ around 0.1, i.e. $u = 34.3$ m/s, we see, that the intensity of the quadrapole terms are approximately one percent of the dipole terms, i.e.

$$I_Q \sim 0.01\, I_D.$$

Thus, we focus on the dipole sources as the relevant terms for noise generation, rather than the quadrapole sources in the turbulent flow field. This means, that we focus on the pressure fluctuations on the solid surface, e.g the side window as the dominant cause for the noise generation.

3 THE GENERIC SIDE MIRROR

To understand the nature of a phenomenon, it is well known that one has to start with a simple model, in order to reduce the complexity of the system. This was definitely one reason for Höld, Brenneis and Eberle[4] and Siegert, Schwarz and Reichenberg[5] to use a simple test geometry, i.e. the quarter of a sphere mounted on a half-cylinder, as a simple model for a side mirror. By all means, they enriched the field of CAA by a simple test case, augmented with ample measurements, which declares the popularity of this model.

We follow this path, using the proposed test case and the measurements to evaluate our computational results.

3.1 Geometry and test case

We start from the generic side mirror model, assembled from a half cylinder with the diameter $d = 0.2m$ and height $h = d$ covered by a quarter sphere and mounted on a plate. As an own part, we establish a special face as part of the plate, which can be regarded as a generic side window. This face will be used in the following as the part where we assemble the pressure fluctuations, i.e. which serves to evaluated the quality according to the mirror geometry. The geometry itself and their position on the plate is shown in Fig. 1.

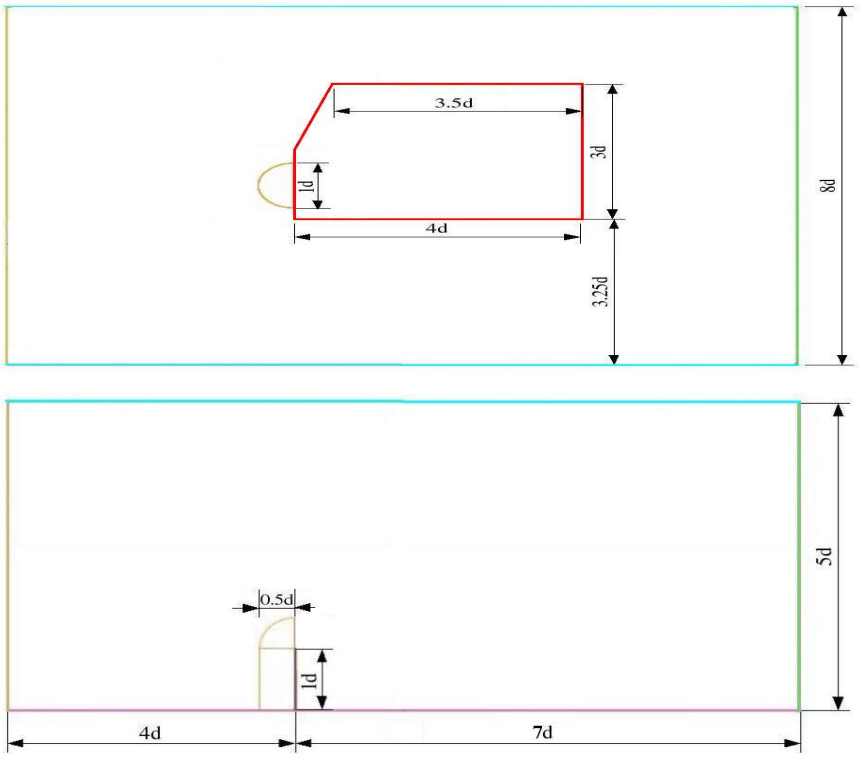

Figure 1: Geometry of the test case $d = 0.2$ m

The free stream velocity of 38.9 m/s is equivalent to a vehicle speed of 140 km/h, which correspond to a Reynolds number of approximately 5×10^5 for this test case. The lateral boundaries are free stream or symmetry boundaries and at the outlet we impose a pressure of 1 atmosphere, i.e. 101325 Pa.

3.2 Meshing strategy

One goal is to find a proper mesh generation process for the geometry description. Since we want to evaluate different geometries under similar conditions, two different approaches are examined. These approaches are:

- a pure hex-mesh
- a hybrid mesh with an outer hex-mesh and an inner box surrounding the mirror. The inner box consists of tetrahedron elements and prism layers, which are located on the mirror surface and the plate.

In Fig. 2 cut planes through the domain of the pure hexa as well as the hybrid mesh are represented.

The advantage of the hybrid approach is the flexibility of the meshing process: One only needs to mesh the box surrounding the mirror, and does not have to care about the outer region. Thus, altering the geometry of the mirror only leads to a re-meshing of the interior box. Thinking in long terms, this is also a practical way to generate an automated optimisation loop for the mirror shape.

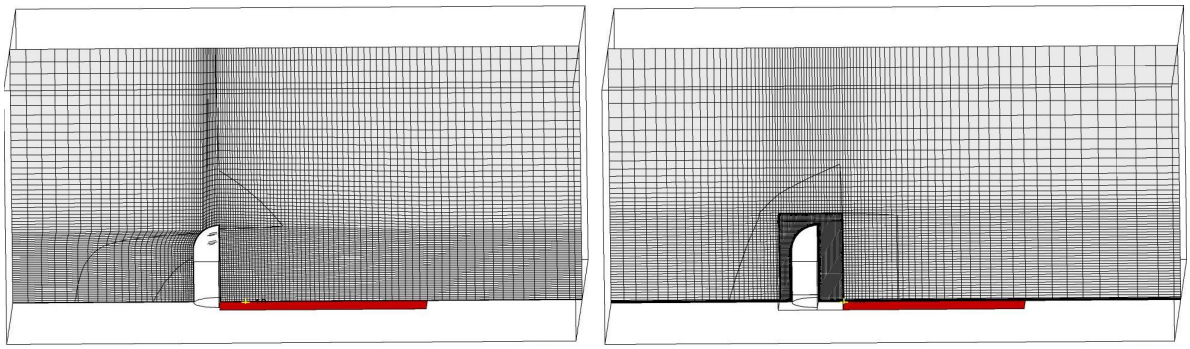

Figure 2: The different mesh strategies: a) hex-mesh on the left b) hybrid mesh on the right

3.3 Turbulence models

Since we are interested in computing the aero acoustic noise sources we have to guarantee an appropriate resolution of the vortex structure of the flow field. Thus, this means that one has to think about a suitable turbulence model to resolve the small scale oscillations, stemming from the fluctuating behaviour of the in-stationary flow. This is always a balance between resolution, chosen turbulence model and computation time.

However, working experience as well as literature studies show, that a simple URANS (Unsteady Reynolds-Averaged-Navier-Stokes) solution with a standard turbulence model will not resolve the time dependent nature of the flow properly for all relevant scales. It is important, to choose more sophisticated turbulence models.

Thus, an appropriate choice would be a LES (Large Eddy Simulation) to resolve at least the big vortex structures and model only the scales beneath the grid size. Unfortunately, due to computational costs and the need to use the results inside an industrial computation process, i.e. the demand of having accurate results in acceptable time, LES modelling seems not to be the resort of first choice.

On the other hand, standard turbulence models like $k-\varepsilon$, $k-\omega$ and the SST-model are not really suitable for aero acoustic computation. Thus we focus on hybrid method like DES (Detached Eddy Simulation) by Spalart *et al.*[6] and SAS (Scale Adaptive Simulation) by Menter and his co-workers[7,8,9]. Both turbulence models posses the benefit to resolve 'detached' eddies, while wall-attached eddies are modelled. Furthermore, the SAS-model exhibit the advantage to use an adaptive turbulent length scale.

3.4 Simulation details

As already mentioned, we compute the generic side window mirror on two different meshes - the pure hex-mesh and the hybrid mesh - with the DES and the SAS model. Due to an accurate resolution of hight frequencies, we assume a time step of $\Delta t = 5. \times 10^{-5}$s. Assuming at least four sampling points per wave, we can resolve frequencies up to 5 kHz. On the other hand, to simulate 1 s one need $20,000$ time steps. Simulation time for this simple test case on 32 CPUs take approx. 10 days.

This is far beyond the scope and we have to think about the necessary computation time quite deeply. Naturally, the sampling of the data for averaging should first start after the bulk inlet velocity has fully flushed the computational domain, i.e after $t_{start} \approx 0.06$ s.

The averaging time, one has to take into account based on the typical scale motion, which is the periodic vortex shedding. Since the Strouhal number can be assumed similar to that of a cylinder in a cross flow, i.e.

$$\begin{aligned} St &= \frac{f_s d}{u} \\ &= 0.2, \end{aligned}$$

the representative period is $t_s = 0.03$ s. From this point of view, following like above de Villiers[10], a simulation time of a least ten realisations of the main shedding frequency should be enough, due to the high frequent nature of aero acoustic noise source and practical reasons.

3.5 Computational results

Comparing the results for different measurement points, one sees clearly that the combination of the hybrid mesh approach with the SAS turbulence models shows the best agreement with the measured data. At least, if one focus on the wake of the side mirror geometry. The location of the considered measurement points are represented in Fig. 3.

If we look at the computational results depicted in Fig. 4, for measurement point 19 in the recirculation zone behind the mirror, we have a strong deviation of all computational approaches. For measurement point 20,21,22 in the wake of the mirror, the accordance for the hybrid meshing approach in combination with the SAS model is quite good.

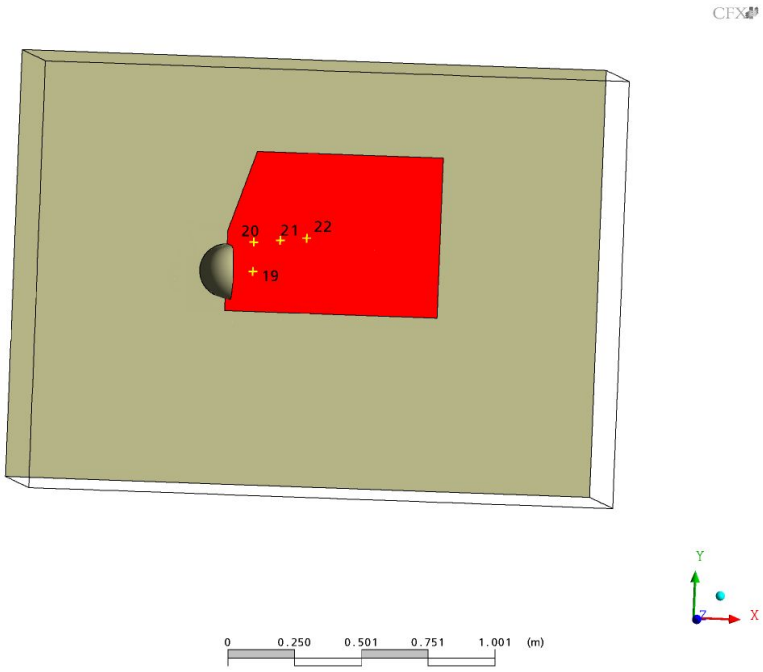

Figure 3: Computational domain with measurement points on the side window

Since we are interested in evaluating the noise sources at the area of the side window, i.e. in the wake of the flow, we focus in the following on the combination of hybrid meshing and the SAS turbulence model.

4 GEOMETRY VARIATION

The intention of this work is not only to recover some measurements to evaluate a computational process. The main focus is to develop a process of computing and especially evaluating different geometries and ranking them. Thus, one important point is to quantify the noise generated by a geometry in a reliable way. So the interesting question is, whether one can forecast noise reduction due to geometric changes by simulation.

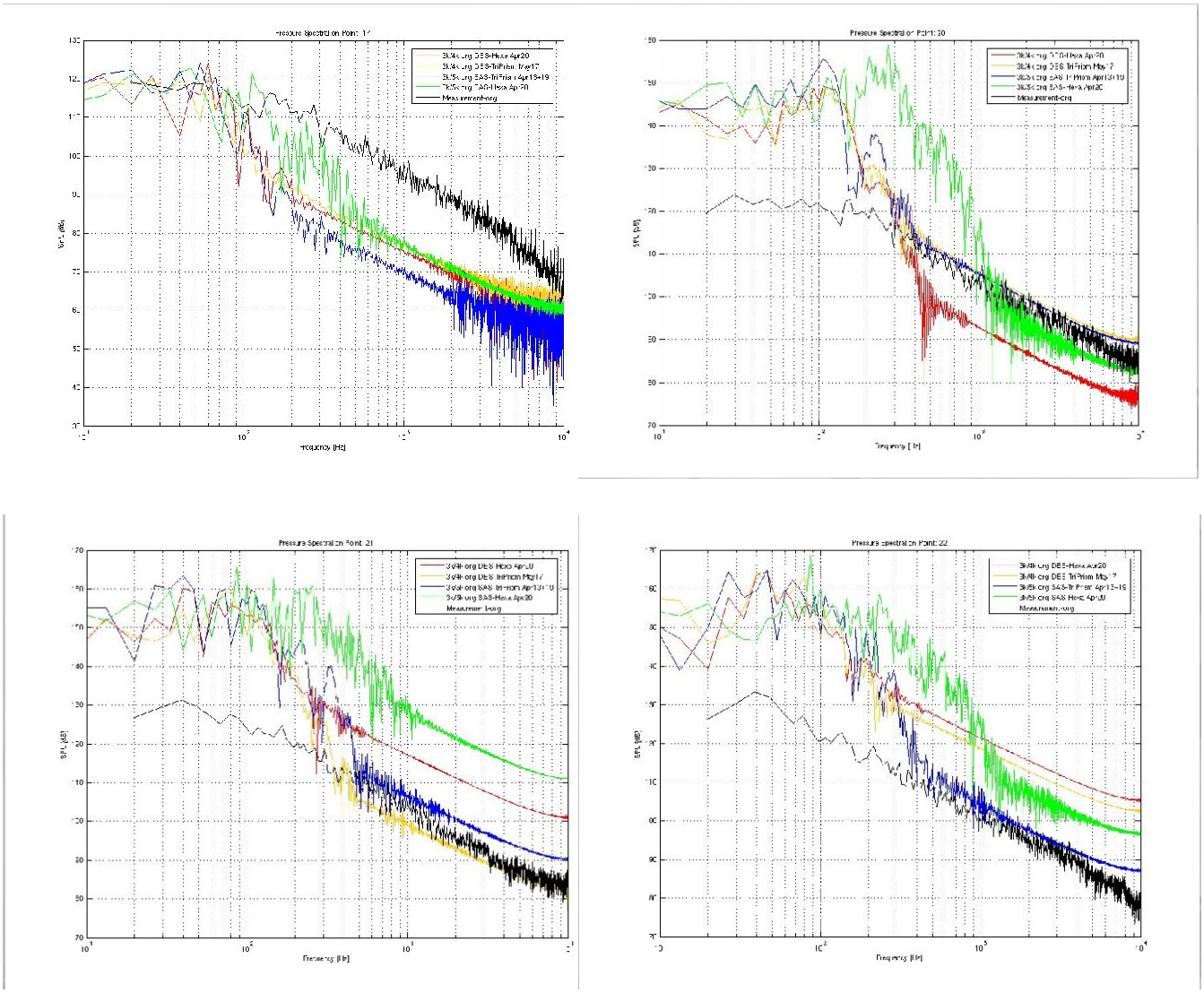

Figure 4: Computational results for measurements point 19, 20, 21 and 22 placed top left, top right, down left and down right, respectively

To build and especially to understand such a process, we start with different geometries, based on the original geometry, only varied by few parameter. Due to discussion with design engineers at Volkswagen, we focused on three parameters which are most important to noise generation from a side mirror.

4.1 Computational process chain

The first intention of this computational process was to rebuild the whole design process automatically, i.e. setting up an automated optimisation routine, build by an automatic meshing, automated pre-processing and parallel computation on our linux cluster. Such

a process chain is well established in our development process and easy to adapted to the aero acoustic calculation. A suitable strategy for the process chain is the following:

- geometry export from the design environment (e.g. ProE, Catia),
- batch meshing with IcemCFD of the inner box/mirror shape
- automated submitting to the parallel cluster
- evaluating the processed data
- changing the design parameter of the parametrised design model

The principal work flow of this process chain is loop depicted in Fig. 5.

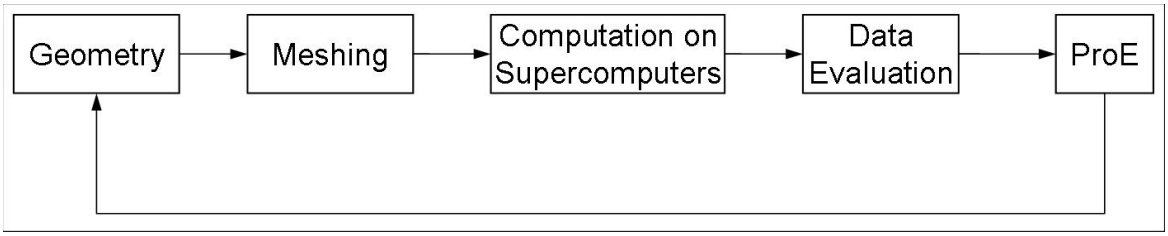

Figure 5: Work flow for an automated process chain

Nevertheless, the problem remains for the computational time which is necessary to resolve the physical relevant features. Since an aero acoustic calculation with a sophisticated turbulence model last also on a parallel cluster several days or weeks, due to the amount of grid cells one has to spend in order to resolve the desired frequencies. Thus, as this work is method development we abandon the idea of an automatic computation and evaluation and start from distinct geometries in order to develop an reliable evaluation process.

4.2 Parametrised model

In order to circumvent the problem computing several month on an parametrised model, we start from three distinct geometries, based on the parametrised model represented in Fig. 6. Due to the working knowledge of the design department and experiments, we focus on the most important parameters for mirror geometries. These parameter are:

- foot height
- foot width
- diffuser angle.

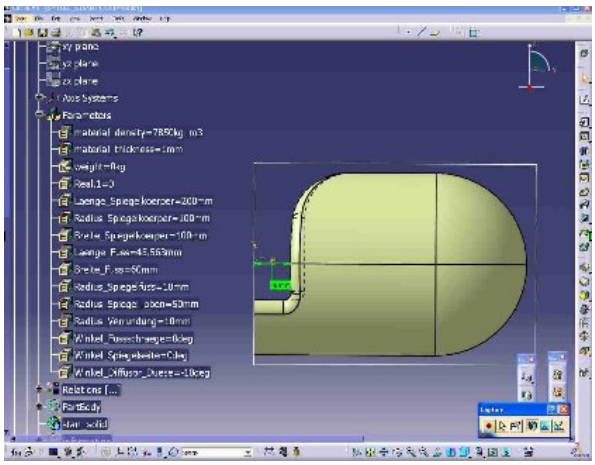

Figure 6: Generic side mirror as a parametrised design model

Concentrating on three modified geometries, we have chosen one geometry possessing all *good properties* (i.e. small foot height, big foot with, and distinct diffuser angle) and one with all *poor properties* (big foot height, small width and no diffuser). The list is completed by a geometry which has values in-between these ranges and the original side mirror. The geometries are depicted in Fig. 7. In Table 1 the parameter of the chosen

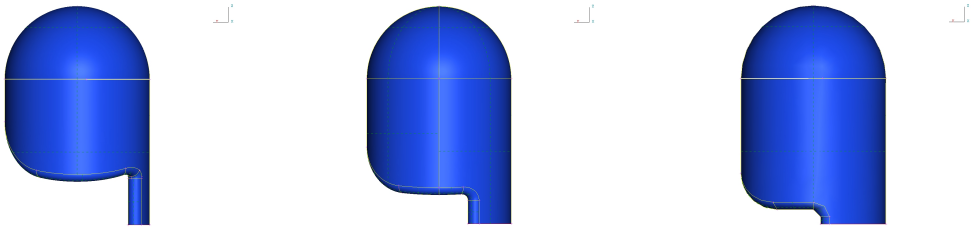

Figure 7: Paramatrised geometries – 306020 (left), 604010 (middle) and 902000 (right)

parametrised models are represented.

properties	foot height [mm]	foot width [mm]	diffuser angle[degree]	name
original	0	0	0	org
poor	90	20	0	90-20-00
in-between	60	40	10	60-40-10
good	30	60	20	30-60-20

Table 1: Parameter of the three modified mirrors

4.3 Evaluation strategy

To find a reliable process to rank different geometries due to their noise production, we focus on the area of the side window as an evaluation surface. This is reasonable since

this is the part, where the noise propagating to the driver's ear passing at first from the outer region to the cabin.

We already motivated why we focus only on the acoustic dipole sources, i.e. the pressure fluctuation p' on the side window. In CFX one can export the acoustic dipoles on a part directly for each time step.

Since we have records for each node on the considered part, we are able to compute the mean pressure fluctuation for each grid point, i.e.

$$p' \;=\; \sqrt{\frac{1}{T}\int_0^T (p(t)-\overline{p})^2\,dt}.$$

Thus, this is the *root mean square of the pressure fluctuation*. Integrating this values over the relevant part and dividing by the area leads to the *mean pressure fluctuation* for the side window i.e.

$$\hat{p} \;=\; \frac{1}{area_{part}}\int_{part} p'\,d\mathbf{x}. \tag{7}$$

From this, one is able to compute the mean sound pressure level of the side window, which gives a measure for the pressure fluctuation on the side window, i.e. the loudness or noisiness of the considered geometry.

4.4 Computational results

The boundary conditions, meshing strategy simulation detail, e.g. time step size and computation time, we adapted from the original generic side mirror. The dipole data, i.e. pressure fluctuation on the side window, can be written in CFX directly for the part. This were done for every time step. After the computation is completed the data are processed in the way described above. This leads to an evaluation process, assigning every geometry with an value for the pressure fluctuation or mean sound pressure level as well as a visual representation of the noise generated on the side window by the mirror geometries. In Fig. 8 the evaluation of the different geometries for the deviation from the mean pressure fluctuation is represented. In Table 2 we find the according values of the minimum, maximum and mean of the deviation from the mean pressure of the side window.

	$\min \tilde{P}[Pa]$	$\max \tilde{P}[Pa]$	mean $\tilde{P}[Pa]$	ranking
original mirror	3.18	272.41	74.50	4.
90 20 00 mirror	2.32	300.62	67.01	3.
60 40 10 mirror	2.43	257.31	56.84	2.
30 60 20 mirror	1.36	176.22	30.68	1.

Table 2: Deviation from the mean Pressure fluctuation on the side window

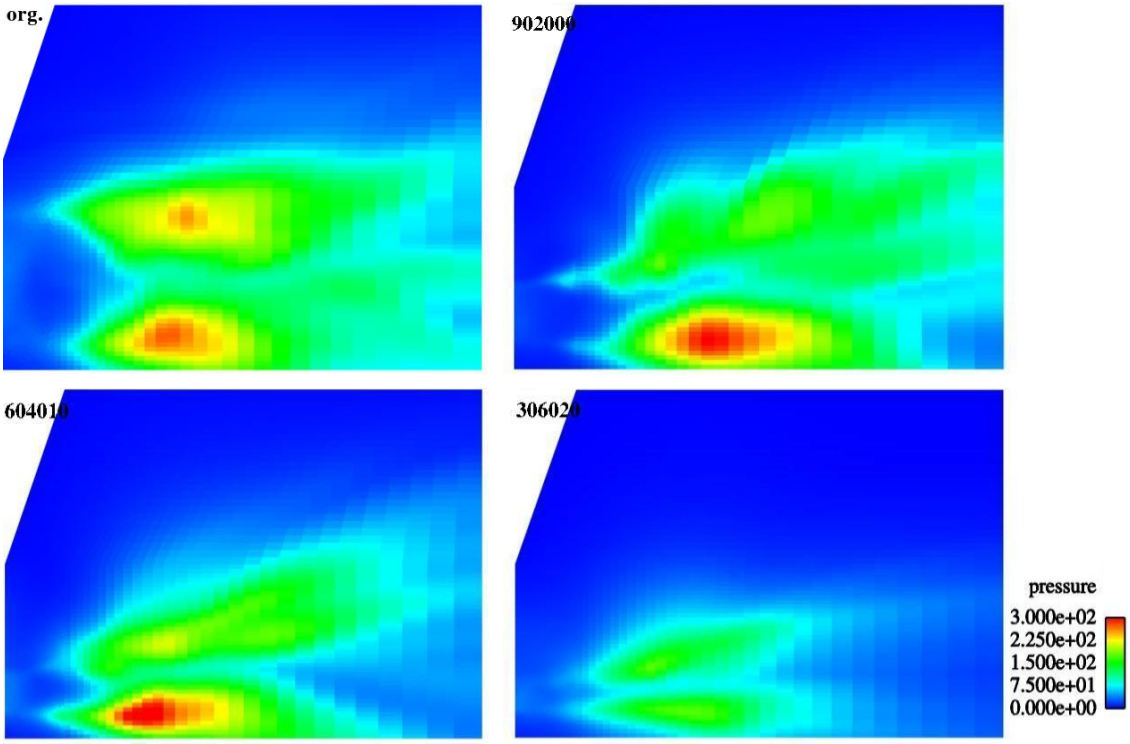

Figure 8: Distribution of the mean pressure fluctuation on the side window for the considered geometries

	min $SPL[db]$	max $SPL[db]$	mean $SPL[db]$	ranking
original mirror	104.04	142.69	127.26	4.
90 20 00 mirror	101.31	143.54	125.11	3.
60 40 10 mirror	101.71	142.19	123.20	2.
30 60 20 mirror	96.64	138.90	117.24	1.

Table 3: Mean sound pressure level on the side window

Clearly, the original mirror has the highest mean pressure fluctuation. Even the minimum deviation from the mean pressure fluctuation on the side window is the biggest for this mirror. Even though the maximum deviation is bigger for the 902000-mirror – the one with the *bad* properties – this one has less mean deviation. The best ratings in all categories posses the 306020-mirror – the one with all *good* properties. Thus, the ranking of the mirror geometries is clear and the working knowledge of the design is approved by our developed evaluation process impressively.

Naturally, since the data from the mean sound pressure level stemming from the pressure data, this result is confirmed by this data. Furthermore, one is able to assign a noise measure – the mean sound pressure level – in $[dB]$ to the single geometry. This measure confirms the above ranking. The plots for the deviation from the mean sound pressure level are shown in Fig. 9 and the values deviation from the mean sound pressure averaged

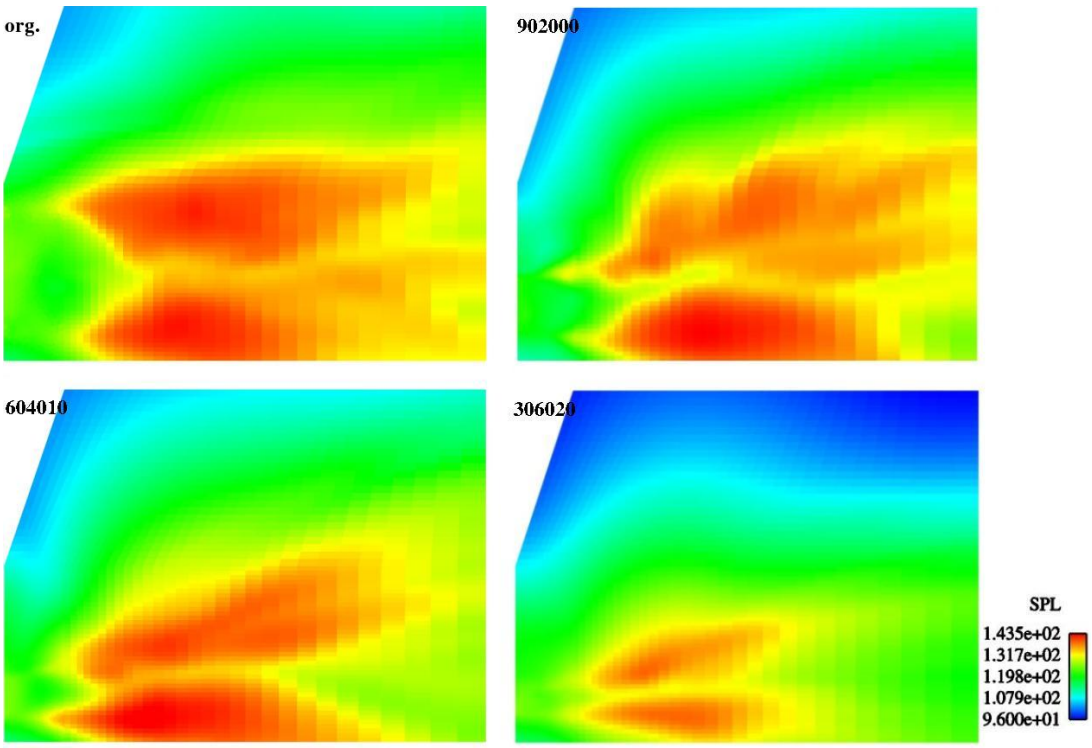

Figure 9: Distribution of the mean sound pressure level on the side window for the considered geometries

over the side window in Table 3.

5 CONCLUSIONS

We applied two different meshing strategies in combination with two different turbulence models – DES and SAS – to a generic side mirror test case and compared the computational results with measurements. Here, the combination of the hybrid mesh with the SAS model showed the best accordance to the data.

Based on this outcome we applied this combination to three different mirror geometries in order to develop an reliable evaluation process to estimate the loudness or noisiness of a mirror geometry. To this use we focused on the pressure fluctuation on the side window part. Here we processed the data and computed the mean deviation of the mean pressure fluctuation. Integrating this over the side window serves as measure of the acoustic property of the geometry.

As this examination is a starting point of such considerations, the outcome was quite satisfying. We reproduced the ranking of the mirror geometries given by our design department. Thus, this seems to be a possible way to build an acoustic evaluation strategy.

Nevertheless, much work has to be done in the future. The next step will be to apply this process to a part model of a real car and side mirror geometry. Here we have own measurements and going to compare this to the ranking which we get from these

evaluation process. Another issue is the computational time which is actually to long for an industrial application process.

REFERENCES

[1] M. J. Lighthill. On sound generated aerodynamically, I General theory. *Proc. Roy. Soc.*, **A 211**, 564–587, (1952).

[2] N. Curle. The influence of solid boundaries upon aerodynamic sound. *Proc. Roy. Soc.*, **A 231**, 505–514, (1955).

[3] J. E. Ffowcs Williams and D. L. Hawkins. Sound generation by turbulence and surfaces in arbitrary motion. sound. *Philos. Trans. Roy. Soc.*, **A 264**, No. 1151,321–342, (1969).

[4] R. Höld, A. Brenneis and A. Eberle. Numerical simulation of aeroacoustic sound generated by generic bodies placed on a plater: Part I - prediction of aeroacoustic sources. in *5th AIAA/CEAS Aeroacoustic Conference. Seattle, Washington*, 10-12 May AIAA-99-1896, (1999).

[5] R.Siegert, V. Schwarz and J. Reichenberger. Numerical simulation of aeroacoustic sound generated by generic bodies placed on a plater: Part II - prediction of radiated sound. in *5th AIAA/CEAS Aeroacoustic Conference. Seattle, Washington*, 10-12 May AIAA-99-1895, (1999).

[6] P. Spalart, W.-H. Jou, M. Strelets and S. R. Allmaras. Comments on the feasibility of LES for wings, and on a hybrid RANS/LES approach. In *Advances in DNS/LES*First AFOSR International Conference on DNS/LES, Greyden, (1997).

[7] F. Menter, M. Kuntz and R. Bender. A scale-adaptive simulation model for turbulent flow prediction AIAA-2003-0767, Reno, NV, (2003).

[8] F.R. Menter and Y. Egorov. Revisiting the turbulent length scale equation. In *IUTAM Symposium: One Hundred Years of Boundary Layer Research*, Göttingen, (2004).

[9] F.R. Menter and Y. Egorov. A scale-adaptive simulation model using two-equation models. AIAA-20051095, Reno, NV, (2005).

[10] E. de Villiers. The potential of large eddy simulation for the modeling of wall bounded flows. PhD thesis, Imperial College London (2005).